Theoretical estimations of third-order optical nonlinearities for semiconductor carbon nanotubes



1999 J. Phys.: Condens. Matter 11 3065

(http://iopscience.iop.org/0953-8984/11/15/012)

J. Phys.: Condens. Matter **11** (1999) 3065–3074. Printed in the UK PII: S0953-8984(99)99890-9

# Theoretical estimations of third-order optical nonlinearities for semiconductor carbon nanotubes

Vl A Margulis†

Department of Physics, NP Ogarev Mordovian State University, Saransk 430000, Russia

Received 3 December 1998

**Abstract.** In this study we present theoretical predictions concerning the third-order nonlinear optical properties of semiconductor carbon nanotubes for photon energies well below the fundamental absorption edge. Both virtual interband $\pi$-electron transitions and combined intraband–interband ones are assumed to be the basic microscopic mechanisms of optical nonlinearities in this spectral region. Resting upon simple dimensional considerations and using only model-independent properties of the $\pi$-electron energy spectrum near the conduction- and valence-band edges, we obtain theoretical estimations for the low-frequency third-order susceptibility $\chi_e^{(3)}(0)$ due to these two mechanisms, which sheds light on the relationship between the non-resonant nonlinear optical response of nanotubes and their geometrical and electronic structure. This result derived in physically interpretable terms is in good agreement with that obtained in our recent study on the basis of a systematic analytical approach. We find that single-shell 'zig-zag' nanotubes display positive $\chi_e^{(3)}(0)$ values, which is due to the positive contribution from combined $\pi$-electron transitions dominating the negative contribution from purely interband transitions. We also find that the increase of the nanotube radius $R$ results in a strong enhancement ($\propto R^4$) of $\chi_e^{(3)}(0)$, which can reach values larger by several orders of magnitude than those reported for the fullerene molecules $C_{60}$ and $C_{70}$. We draw a conclusion that the modification of the geometrical structure of nanotubes provides an efficient means for the engineering of novel nonlinear-optical materials with high cubic susceptibilities.

## 1. Introduction

The study of carbon nanotubes (CNs) is now an active area of research, which can lead to the development of advanced technological devices. Despite the progress achieved in this field during the last few years (for reviews, see [1–4]), a number of physical properties of CNs have not been examined carefully so far. In particular, this applies to the nonlinear optical (NLO) properties of CNs, which determine the nonlinear dependence of the polarizability of CNs on the intensities of incident electromagnetic waves. To our knowledge, experiments on the measurement of this dependence have not yet been conducted. Meanwhile, such experiments have been performed for condensed phases $C_{60}$ and $C_{70}$ [5–12] and have exhibited interesting NLO behaviours of these two fullerene molecules. Theoretical NLO response calculations on the fullerenes $C_{60}$ and $C_{70}$ have been carried out by a number of authors [13–16] and are found to be in good agreement with the experimental data of Wang and Cheng [6] and of Kafafi *et al* [10, 11]. In the near future such an experimental study is expected to be performed for CNs, which are fullerene-related materials. Therefore, it may be worthwhile to present theoretical

† Correspondence address: Sovetskaya 31, kv. 32, Saransk 430000, Russia.

0953-8984/99/153065+10$19.50  

information on the NLO properties of CNs, which would allow one to assess CNs from the viewpoint of their possible applications in optic and opto-electronic devices.

The first step towards this aim has been made in our previous work [17], in which a systematic analytical approach to NLO properties of single-shell semiconductor CNs has been proposed. This approach was applied for the calculation of the susceptibility $\chi^{(3)}(\omega)$, which is responsible for third-order NLO effects such as the optical Kerr effect, third-harmonic generation and degenerate four-wave mixing. It has been shown that the large values of $\chi^{(3)}$ obtained along with the unique character of its frequency dependence in the transparency region make CNs very attractive for practical purposes. It should be noted, however, that a complete treatment of the above mentioned effects is not particularly simple and requires cumbersome calculations based on the Genkin–Mednis perturbation theory technique [18], most of which have been done numerically. Besides, this approach does not provide any deep insight into the problem and is unable to explain the true nature of the relationship between optical nonlinearities of CNs and characteristic parameters of their geometrical an electronic structure. In this respect, a simple formulation shedding light on the NLO properties of CNs in physically interpretable terms might be useful.

Our aim in this paper is to propose such a formulation. The approach we develop here rests upon physical intuition and uses only dimensional considerations and model-independent properties of the $\pi$-electron energy spectrum near the band edges in semiconductor CNs. The advantages of this approach are obvious. First, it allows one to obtain an explicit expression for the off-resonance third-order optical susceptibility $\chi_e^{(3)}(0)$ of CNs in a considerably simpler fashion than other methods do. Secondly, it gives a clear physical picture of the processes involved, clarifying the effect upon $\chi_e^{(3)}(0)$ of changing the circumference length of the tubules and the width of the bandgap in their $\pi$-electron energy spectrum. One of the most remarkable features of CNs we recover based on this approach is that the geometry of these tubules plays a fundamental role in determining their NLO properties. We find that it is just the nanotube radius—the geometrical parameter which specifies the tubular circumference—that mainly controls the magnitude of $\chi_e^{(3)}(0)$. In particular, the increase of the parameter results in strong enhancement of $\chi_e^{(3)}(0)$. This behaviour leads to very large values of $\chi_e^{(3)}(0)$ which are larger by several orders of magnitude than those reported for the fullerene molecules $C_{60}$ and $C_{70}$ in condensed phases. The findings indicate that CNs possess a significant potential for applications to nonlinear optical devices.

The outline of the paper is as follows. The geometrical and electronic structure of CNs is reviewed in section 2. In section 3 a simple physical picture of the nonlinear response of CNs in a two-band approximation is provided and theoretical estimations for $\chi_e^{(3)}(0)$ are presented. In section 4 we discuss the obtained results and the experimental implications of the findings. Finally, in section 5 we present the conclusions.

## 2. Tubule models

We concern ourselves with an idealized system which consists of an array of identical, single-shell and open-ended CNs that have their axes parallel to each other. The widely used model of such tubules is a semi-infinite sheet of graphene rolled up into a cylinder of a constant radius. The structure of a nanotube is specified by a chiral vector

$$\boldsymbol{C} = n_1\boldsymbol{a}_1 + n_2\boldsymbol{a}_2 \tag{1}$$

where $n_1$ and $n_2$ are integers, and $\boldsymbol{a}_1$ and $\boldsymbol{a}_2$ are the primitive lattice vectors of a two-dimensional (2D) graphite sheet (figure 1). A set of two integers $(n_1, n_2)$ uniquely determines the type of

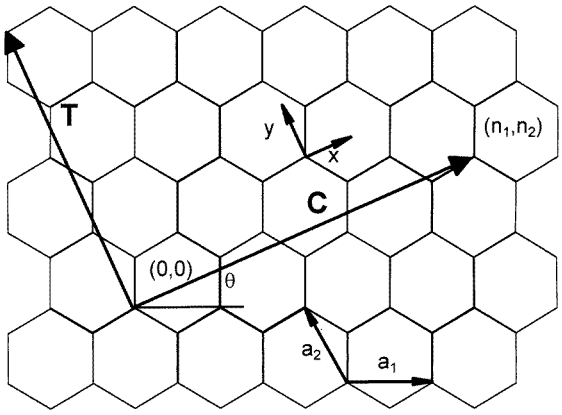


**Figure 1.** Fragment of a two-dimensional graphite sheet which is rolled up in order to construct a nanotube specified by a pair of integers $(n_1, n_2)$. The unit vectors denoted by $\boldsymbol{x}$ and $\boldsymbol{y}$ are directed along the circumference and the axis of a nanotube, respectively. Also shown are a chiral vector $\boldsymbol{C}$ and a fundamental lattice vector $\boldsymbol{T}$ along the direction of the tube axis.

nanotube, the tubule radius $R$ and the chiral angle $\theta$ being defined as

$$R = \frac{a_0}{2\pi}(n_1^2 + n_2^2 - n_1 n_2)^{1/2} \tag{2}$$

$$\theta = \tan^{-1}[\sqrt{3}n_2/(2n_1 - n_2)]. \tag{3}$$

Here $a_0 = \sqrt{3}d_0$ is the lattice constant of the graphite, the carbon–carbon (C–C) bond length being $d_0 = 1.42$ Å.

Among the different possible directions of rolling up the graphite sheet there are two singled-out directions for which the superposition of the original hexagon $(0, 0)$ with the hexagon $(n_1, n_2)$ is not accompanied by a distortion of the structure of the latter. These two special cases corresponding to the chiral angles $\theta = 0$ and $\theta = \pi/6$, respectively, give rise to highly symmetric structures of two types, namely, to the $(n, 0)$ 'zig-zag' nanotubes for which two C–C bonds of each carbon hexagon are parallel to the tube axis, and to the $(2n, n)$ 'arm-chair' nanotubes for which two C–C bonds of each hexagon are perpendicular to the axis. According to the theoretical predictions [19–27], the radius of the nanotube and the arrangement of the carbon atoms in its shell determine whether the nanotube possesses metallic or semiconducting properties. Thus, for instance, the arm-chair tubes are metallic, whereas zig-zag tubes are semiconductors. Our further consideration is restricted to semiconductor nanotubes only. For a more detailed classification of this type of tubule it is convenient to introduce two integers $p$ and $q$ connected with the integers $n_1$ and $n_2$ by means of the relation $n_1 - 2n_2 = 3q + p$. As shown in [28–30], the tubules with $p = 0$ and $q \neq 0$ are narrow-gap semiconductors, whereas the tubules with $p = 1, 2$ and with an arbitrary $q$ are moderate-gap semiconductors.

To describe the electronic structure of semiconductor CNs we use the model proposed in [27] on the basis of the $\boldsymbol{k} \cdot \boldsymbol{p}$ perturbation scheme. Within the framework of this model the electron-energy spectrum in the lowest conduction band (c band) and in the highest valence band (v band) can be obtained from the effective Hamiltonian [17]

$$H_{\text{eff}} = (\Delta_g/2)\sigma_x - \mathrm{i}\gamma\nabla_y\sigma_y \tag{4}$$

where $\sigma_x$ and $\sigma_y$ are Pauli spin matrices, $\Delta_g$ is the bandgap energy in the $\pi$-electron spectrum, and $\gamma$ is the $\boldsymbol{k} \cdot \boldsymbol{p}$ interaction constant connected with the transfer integral $t_0 = -3.03$ eV

[20, 21] between the $\pi$-orbitals of the nearest-neighbouring carbon atoms by means of the relation $\gamma = \sqrt{3}|t_0|a_0/2$. Note that equation (4) is written down in Cartesian coordinates with the $x$ and $y$ axes directed along the circumference and the axis of a nanotube, respectively.

The explicit expressions of the electron energy dispersion $\varepsilon_{c,v}(k)$ for the two bands under consideration can be presented in the form

$$\varepsilon_c(k) = -\varepsilon_v(k) = [(\Delta_g/2)^2 + \gamma^2 k^2]^{1/2} \tag{5}$$

where $k$ is the component of the electron wavevector along the tubule axis. Thus, owing to a very small radius of the CNs their energy bands exhibit typical 1D character with a divergent density of states at the band edges. The latter are located at the K points of the hexagonal graphite sheet Brillouin zone (figure 2). Within the zone-folding method these points are mapped onto the $\Gamma$ point of the nanotube 1D Brillouin zone. The bandgap energy $\Delta_g$ at the $\Gamma$ point ($k = 0$), is expressed as follows [28–31]

$$\Delta_g = (t_0 d_0/R)[1 + (-1)^p (d_0/12R)\cos\theta] \tag{6}$$

where the second term is square brackets takes into account the dependence of $\Delta_g$ on the chiral angle $\theta$ for the moderate-gap semiconductor CNs ($p = 1, 2$). This term originates from $\sigma$–$\pi$ hybridization, which, in its turn, is due to the effect of the curvature of nanotubes. As shown in [28–30], for CNs with not very small radius ($R > 4$ Å) the second term in equation (6) presents but a small correction to the first one and it can be neglected without sacrificing much accuracy.

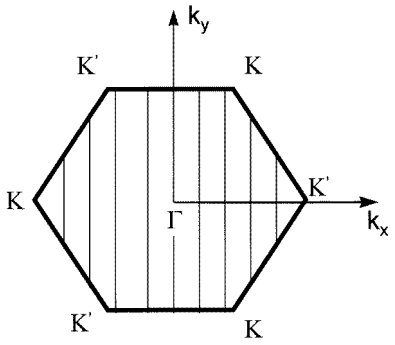


**Figure 2.** The first Brillouin zone of the graphite sheet. The discrete lines show the allowed values of the electron wavevector $\boldsymbol{k}$.

Note that although the $R^{-1}$ behaviour of the gap $\Delta_g$, the same as equation (5) for the $\pi$-electron energy spectrum near the valence- and conduction-band edges, has been obtained within the $\boldsymbol{k}\cdot\boldsymbol{p}$ approximation by using strongly simplifying assumptions, they remain in force in evaluating the electronic structure of CNs also be means of other methods, in particular by the tight-binding method, and in this sense they can be viewed as being model independent.

## 3. Third-order optical susceptibility of nanotubes in the low-frequency limit

We turn now to the evaluation of the nonlinear response of a bundle of identical and equally oriented zig-zag nanotubes $(n, 0)$ to the external electromagnetic field polarized parallel to their axes. The structure of such nanotubes is described by the point symmetry group $D_{nh}$ or $D_{nd}$ for even and odd $n$, respectively [32, 33]. Since inversion is an element of symmetry of these groups, it is just the $\chi^{(3)}(\omega)$ which is the lowest-order nonvanishing susceptibility in

the dipole approximation. At frequencies many times higher than the infrared frequencies of the lattice vibration, the main contribution to $\chi^{(3)}(\omega)$ originates from the delocalized $\pi$-band electrons, the motion of which may be viewed at a fixed lattice ion configuration. Then, within a single-electron approach the full response of the system to the external AC electromagnetic field can be obtained by the summation of response of all the electrons with regard for the Pauli exclusion principle.

In the dipole approximation the interaction Hamiltonian of the electron with the electromagnetic field is given by

$$\boldsymbol{H}_{int} = -\boldsymbol{d}\boldsymbol{E}(t) = e\boldsymbol{r}\boldsymbol{E}(t) \tag{7}$$

where $\boldsymbol{d}$ is the operator of the electric dipole moment of one electron, and $\boldsymbol{E}(t)$ is the strength of the electric field of an incident wave. From the band theory formalism it is well known that the operator of the electron coordinate $\boldsymbol{r}$ in the crystal momentum representation is separated into two parts as follows:

$$\boldsymbol{r} = \mathrm{i}\nabla_{\boldsymbol{k}} + \mathrm{i}\boldsymbol{X}. \tag{8}$$

The first part in the right-hand side of the above equation describes the motion of the free electron in the band $s$ characterized by the energy dispersion law $\varepsilon_s(\boldsymbol{k})$, whereas the second part is expressed in terms of the transition matrix

$$X_{ss'}(\boldsymbol{k}) = \int u^*_{s\boldsymbol{k}}(\boldsymbol{r})\nabla_{\boldsymbol{k}} u_{s'\boldsymbol{k}}(\boldsymbol{r})\,\mathrm{d}\boldsymbol{r} \tag{9}$$

which couples a pair of electronic states, one in band $s$ and the other in band $s'$ with wavevector of $\boldsymbol{k}$. Here $u_{s\boldsymbol{k}}(\boldsymbol{r})$ is the periodic part of the Bloch wave function $\psi_{s\boldsymbol{k}}(\boldsymbol{r}) = u_{s\boldsymbol{k}}(\boldsymbol{r})\exp(\mathrm{i}\boldsymbol{k}\cdot\boldsymbol{r})$. The integration in equation (9) extends over the unit cell, which presents the rectangle defined by the chiral vector $\boldsymbol{C}$ and the translation vector $\boldsymbol{T}$ (see figure 1), the latter being equal to $\boldsymbol{a}_1 + 2\boldsymbol{a}_2$ for zig-zag nanotubes.

From equations (7)–(9) it follows that there are two distinct electronic contributions to the electric dipole moment of the system. The first of them is associated with intraband electron motion under the action of the applied field, i.e. the electric field of the light wave. The second contribution arises from the virtual interband transitions induced by the external field and occurring between only states of the same $\boldsymbol{k}$ value in different bands. Consequently, there are three main electronic mechanisms that lead to the third-order NLO response, namely, the motion of free electrons in partially occupied bands, virtual electron transitions across the bandgap and, finally, the combined motion of electrons associated with intraband–interband transitions. Hereafter the subscripts 'intra', 'inter' and 'comb' are used to specify the corresponding contributions to the susceptibility $\chi^{(3)}_e$. It should be noted that for the system under consideration the first of the above mentioned contributions, $\chi^{(3)}_{\mathrm{intra}}$, can be neglected. The reason is that for the real single-shell CNs, the diameters of which range typically between 7 and 15 Å, the bandgap energy $\Delta_g$ is much greater than the thermal energy $k_BT$. In this case the electron occupation for the conduction band states will be determined by the doping level of CNs. Hence, for undoped semiconductor CNs the v band will be fully occupied, whereas the c band will be quite empty even at room temperature. Thus, the intraband contribution to $\chi^{(3)}_e$ vanishes and we can write

$$\chi^{(3)}_e(\omega) = \chi^{(3)}_{\mathrm{inter}}(\omega) + \chi^{(3)}_{\mathrm{comb}}(\omega). \tag{10}$$

For incident photon energy well below the fundamental absorption edge ($\hbar\omega \ll \Delta_g$), the susceptibilities in equation (10) will not depend on the frequency $\omega$ at all and theoretical estimations of the first and second terms of equation (10) can easily be obtained on physical grounds.

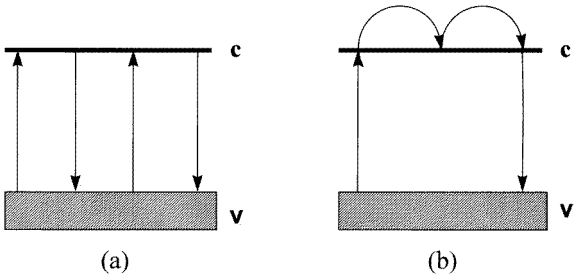


**Figure 3.** A schematic representation of the excitation pathways contributing to the third-order optical susceptibility $\chi_e^{(3)}(0)$ in a two-band model of the electronic structure of CNs. (a) Shows the purely interband excitations and (b) shows the combined intraband–interband ones.

Let us consider first the contribution to $\chi_e^{(3)}$ associated with purely interband transitions (figure 3(a)). In estimating $\chi_{\text{inter}}^{(3)}$ we must take into account two parameters which are relevant to the NLO process, namely, the frequency $\omega_{cv}$ of the above mentioned transitions and the part of the dipole moment $d_{cv}$ arising from the matrix element $X_{cv}$ of the lattice-periodic operator $\boldsymbol{X}$. Based on simple dimensional considerations we then obtain in the low-frequency approximation

$$\chi_{\text{inter}}^{(3)}(0) \approx -\frac{N}{V}\frac{d_{cv}^4}{(\hbar\omega_{cv})^3} \approx -\frac{N}{V}\frac{(eX_{cv})^4}{\Delta_g^3} \tag{11}$$

where $N/V$ is the number of unit cells per unit volume.

The negative sign of the susceptibility $\chi_{\text{inter}}^{(3)}(0)$ is prompted by the following parallel which makes this result understandable. As already noted, the virtual interband excitations in our model effectively couple only specific pairs of states, namely, only states of the same $\boldsymbol{k}$ value in different bands as the photon momentum is negligible. Therefore, as far as the interband contribution to $\chi_e^{(3)}(0)$ is concerned the model under consideration can be represented as a set of independent simple two-level systems with the appropriate (for each value of the wavevector) energy separation between the levels and oscillator strength for interlevel transitions. The electron excitations for each above mentioned pair of allowed $\boldsymbol{k}$ states can be treated then as being completely localized and, therefore, one can expect a negative sign of $\chi_{\text{inter}}^{(3)}(0)$ for a large number of such systems brought together to form a whole [34]. It is for this reason that the minus sign is written in the right-hand side of equation (11). The validity of the above considerations can be confirmed by the evaluation of $\chi_{\text{inter}}^{(3)}(0)$ on the basis of the formalism outlined in [17].

We turn now to the estimation of the dipole transition matrix element $X_{cv}$. As we show below it can be done without recourse to a direct calculation of $X_{cv}$ by using equation (9) (the latter would require detailed information on the electronic states of the CNs), but first it is necessary to make the following remark. Because of the divergence of the joint density of the electronic states $\rho(\omega_{cv})$ at the Brillouin zone centre where the valence- and conduction band edges are located,

$$\rho(\omega_{cv}) = \frac{2}{\pi}\left(\frac{\mathrm{d}\hbar\omega_{cv}}{\mathrm{d}k}\right)^{-1} \propto \frac{1}{\sqrt{(\hbar\omega_{cv})^2 - \Delta_g^2}} \tag{12}$$

the main contribution to $X_{cv}$ arises from the band-edge electron transitions. Since the group of the wavevector at the extremum point of the bands admits inversion as a symmetry operation, the Bloch amplitudes $u_{ck}$ and $u_{vk}$ have opposite parity at this point and can be chosen as entirely

real. From equation (9) it then follows that the matrix element $X_{cv}$ is purely real and satisfies the equation

$$X_{cv}(k) = -X_{vc}(k). \tag{13}$$

Now, to estimate $X_{cv}$ we can make use of the so-called $f$-sum rule for the electric dipole transitions:

$$\frac{m_e}{\hbar^2}\frac{\partial^2\varepsilon_s(k)}{\partial k^2} = 1 + \frac{2m_e}{\hbar^2}\sum_{s'\neq s}[\varepsilon_s(k) - \varepsilon_{s'}(k)]|X_{ss'}(k)|^2 \tag{14}$$

where $m_e$ is the free electron mass. For the two-band model under consideration the sum in the right-hand side of equation (14) contains only one term and from equations (13) and (14) we easily obtain

$$X_{cv} \approx \frac{\gamma\Delta_g}{(\hbar\omega_{cv})^2} \approx \frac{\gamma}{\Delta_g}. \tag{15}$$

Finally, it is not hard to show that for a hypothetical bulk specimen of aligned zig-zag CNs $(n, 0)$ the number of unit cells per unit volume is given by

$$\frac{N}{V} = \frac{n}{2\sqrt{3}\pi^2 R^3}. \tag{16}$$

Now, using equations (6), (11), (15) and (16) we obtain

$$\chi^{(3)}_{\text{inter}}(0) \approx -\frac{(3e)^4 n}{2^5\sqrt{3}\pi^2}\frac{R}{\Delta_g^3} = A_1\frac{(3eR)^4}{\pi^2\gamma^3} \qquad A_1 = -\frac{3^{5/2}}{2^8}n. \tag{17}$$

In a similar fashion, it is easy to estimate the contribution to the susceptibility $\chi_e^{(3)}(0)$ associated with combined intraband–interband transitions. The latter are shown schematically in figure 3(b). As is clear from the diagram in figure 3(b), this contribution originates from both the acceleration term of the coordinate $\mathrm{i}(\partial/\partial k)$ and from the regular interband term $X_{cv}$. The combination of these terms relevant to the third-order NLO susceptibility $\chi^{(3)}_{\text{comb}}(0)$ follows uniquely from the simple dimensional considerations with regard for the physical picture of the processes involved. In the low-frequency limit we have

$$\chi^{(3)}_{\text{comb}}(0) \approx \frac{N}{V}\frac{e^2}{\hbar\omega_{cv}}\left[\frac{\partial}{\partial k}\left(\frac{d_{cv}}{\hbar\omega_{cv}}\right)\right]^2 \approx \frac{N}{V}\frac{e^4}{\Delta_g}\left[\frac{\partial}{\partial k}\left(\frac{X_{cv}}{\hbar\omega_{cv}}\right)\right]^2. \tag{18}$$

In order to make this equation more physically tractable, we prefer to rewrite it as follows

$$\chi^{(3)}_{\text{comb}}(0) \approx \frac{N}{V}\frac{4e^4}{\Delta_g\hbar^2}v^2\left[\frac{\partial}{\partial\omega_{cv}}\left(\frac{X_{cv}}{\omega_{cv}}\right)\right]^2 \tag{19}$$

where $v$ is the electron velocity at the band edge. From the expression, equation (4), for the effective Hamiltonian it follows that $v \sim \gamma/\hbar$. Using equation (15), (16) and (19), we then obtain

$$\chi^{(3)}_{\text{comb}}(0) \approx \frac{(3e)^4 n}{2^3\sqrt{3}\pi^2}\frac{R}{\Delta_g^3} = A_2\frac{(3eR)^4}{\pi^2\gamma^3} \qquad A_2 = \frac{3^{5/2}}{2^6}n. \tag{20}$$

Finally, using equations (17) and (20) in equation (10) yields

$$\chi_e^{(3)}(0) \approx A\frac{(3eR)^4}{\pi^2\gamma^3} \qquad A = \frac{3^{7/2}}{2^8}n. \tag{21}$$

The positive sign of the total susceptibility $\chi_e^{(3)}(0)$ indicates that the combined intraband–interband $\pi$-electron transitions mainly contribute to the NLO response of the CNs.

The predominance of the combined term in $\chi_e^{(3)}(0)$ is easy to understand on the qualitative level. It is the consequence of the rapid variation of the dipole matrix element $X_{cv}(k)$ as $k$ moves away from the Brillouin zone centre where $X_{cv}(k)$ achieves a maximum value (see equation (15)) and where the joint density of the electronic states becomes theoretically finite (see equation (12)). The latter two properties are typical of quasi-1D electron systems, so that the positive sign of $\chi_e^{(3)}(0)$ just reflects the 1D character of the highly delocalized $\pi$-electron system in CNs.

The above estimation of $\chi_e^{(3)}(0)$ is in good agreement with the exact solution for the third-order susceptibility of CNs obtained in our previous study [17] on the basis of the Genkin–Mednis formalism [18]. The analytical result for $\chi_e^{(3)}(0)$ derived in [17] has the form

$$\chi_e^{(3)}(0) = A\frac{(3eR)^4}{\pi^2\gamma^3} \qquad A = A_1 + A_2 = \frac{4}{5} \tag{22}$$

where $A_1$ and $A_2$ are constants equal to $-8/35$ and $36/35$, respectively. It is easy to see that the order of magnitude of these constants is the same as the corresponding factors in equations (17) and (20) with the integer $n \leqslant 20$ typical of single-shell zig-zag nanotubes which are experimentally available at present.

## 4. Discussion

As seen from equations (21) and (22), the low-frequency susceptibility $\chi_e^{(3)}(0)$ can provide information on the main parameters of the geometrical and electronic structure of nanotubes, namely, on their radius $R$ and on the $\boldsymbol{k}\cdot\boldsymbol{p}$ interaction constant $\gamma$, the latter being connected with the interaction energy $t_0$ between the two 2p electrons on the nearest-neighbouring $\pi$ orbitals via the simple relation mentioned in section 3. According to equation (6), it is just these two parameters that determine the width of the band gap $\Delta_g$ in the $\pi$-electron energy spectrum of nonchiral semiconductor CNs. Therefore, if we know the magnitude of one of them we can determine that of the other by measuring the quantity $\chi_e^{(3)}(0)$ and thus determine the bandgap energy $\Delta_g$. Such a method of experimental estimation of the parameters $t_0$, $\gamma$ and $\Delta_g$ may be of interest because the resolution of a modern electron microscope is sufficient for precise measurements of the radii of CNs. Of course, the method suggested here can be used only for rough estimations of the above mentioned parameters, since the present experimental NLO studies in themselves are not able to provide a good enough accuracy.

The most important result we predict on the basis of the obtained equation (21) is considerable enhancement of the magnitude of $\chi_e^{(3)}(0)$ for CNs as compared with those reported for the fullerenes $C_{60}$ and $C_{70}$ in condensed phases. Indeed, a number of authors [6, 10, 11] who have performed measurements of the third-order NLO response of such fullerenes found the off-resonance $\chi^{(3)}$ values to be around $10^{-12}$ esu; the experimental data are very close to those obtained by theoretical calculations [13, 14]. Meanwhile, equation (22) at typical values of the parameters of single-shell CNs ($R = 5.5$ Å and $\gamma = 6.46$ eV) yields $\chi_e^{(3)}(0) \sim 10^{-9}$ esu, i.e. three orders of magnitude larger than for the fullerenes. Such an essential difference in the order of magnitude of $\chi_e^{(3)}(0)$ for such closely related objects as fullerenes and CNs can be attributed to the fact that in fullerene molecules, because of their spherelike geometries, not all the possibilities inherent in the very strongly delocalized nature of the $\pi$-electron states are realized, as is the case for quasi-1D tubular systems. The origin of the very large optical nonlinearity of CNs is accounted for by the coincidence of three peculiarities of their electronic structure at one and the same point of the 1D Brillouin zone, namely, the theoretical infinite joint density of the electron states, the maximum value of the dipole transition matrix element and the

minimum value of the width of the band gap in the $\pi$-electron energy spectrum. In this respect CNs are reminiscent of conjugated chain polymers such as polyacetylene or polydiacetylenes which also exhibit extremely high values of non-resonant third-order susceptibility.

Another remarkable feature predicted by equation (21) is the strong nonlinear dependence of the off-resonance susceptibility $\chi_e^{(3)}(0)$ on the nanotube radius $R$: $\chi_e^{(3)}(0) \propto R^4$. The dependence suggests that one could use it in order to design new NLO materials with enhanced cubic susceptibilities. Thus, for instance, the increase of $R$ by three times as against the above mentioned typical value equal to 5.5 Å leads to the enhancement of $\chi_e^{(3)}(0)$ up to a record figure of the order of $10^{-7}$ esu. From a practical viewpoint it is desirable, of course, that the cubic susceptibility should have the largest possible values in the region far from the single-photon resonance since in this case the optical losses will be minimal and the response time will be the shortest. On the other hand, it should be noted that the growth of $R$—the parameter which mainly governs the optical nonlinearity—leads to a narrowing of the transparency region of nanotubes. However, with the increase of $R$ the narrowing falls off as $R^{-1}$, since the bandgap depends inversely on the tube radius. Hence, the decrease of the transparency region proceeds much more slowly than the increase of $\chi_e^{(3)}(0)$ with $R$. Thus, in order to obtain a larger NLO response of the CNs in the non-resonant regime it is preferable to use nanotubes with a larger radius, of course, under otherwise equal conditions. Therefore, to make progress in the possible applications of nanotubes in different NLO devices one is prompted to develop new methods for fabricating arrays of aligned nanotubes with fairly large radii ($R \sim 15$–$20$ Å) which would allow the NLO response of nanotubes in the transparency region to be optimized.

Finally, it should be stressed that the approach proposed in this paper is valid only in the low-frequency limit when the virtual transitions of $\pi$-electrons are the basic microscopic reasons for the optical nonlinearities of CNs. The approximations we have used lose their force when the frequency of the incident radiation approaches the fundamental absorption edge. In this case, in contrast to that of nonlinearities created by virtual processes, real excited state populations are generated, which leads to a giant enhancement of the NLO signals. In this situation, in order to obtain analytical results for the third-order susceptibility $\chi_e^{(3)}(\omega)$ one should use a more rigorous theory, since qualitative considerations alone are insufficient for the purpose. A detailed treatment of this problem will be given elsewhere [35].

## 5. Conclusions

In this paper we have studied the third-order NLO susceptibility of semiconductor CNs in the spectral region where the optical frequencies are well below the fundamental absorption edge. Our approach is based upon simple qualitative considerations and makes use of only model-independent properties of the $\pi$-electron energy spectrum of CNs near the valence- and conduction-band edges. The advantage of the approach is that it provides a clear physical picture of the processes involved and a deeper understanding of the basic physical mechanisms of the low-frequency optical nonlinearity of CNs. In particular, it enables one to clarify the physical implication of our central result (equation (21)) establishing the relationship between the susceptibility $\chi_e^{(3)}(0)$ and the two characteristic parameters of the geometrical and electronic structure of nanotubes, namely, their radius $R$ and the $\boldsymbol{k} \cdot \boldsymbol{p}$ interaction constant $\gamma$. The above mentioned equation emerging naturally from our considerations is consistent (with the accuracy up to a numerical coefficient) with that obtained previously on the basis of the systematic analytical approach [17]. According to equation (21), the low-frequency susceptibility $\chi_e^{(3)}(0)$ of CNs scales as the fourth power of $R$ and can exceed the corresponding NLO susceptibilities of the fullerenes $C_{60}$ and $C_{70}$ by several orders of magnitude. The results obtained allow one to consider semiconductor CNs as a very promising material for applications in NLO devices.

In order to emphasize the basic physical ideas we have restricted our consideration to nonchiral CNs possessing a centre of inversion. As has been already mentioned, in such systems the even-order susceptibilities vanish and it is just the cubic susceptibility $\chi^{(3)}$ which is the lowest-order nonvanishing nonlinearity. In terms of the future efforts in this field, we believe that investigations of the second-order NLO susceptibility $\chi^{(2)}$ of CNs without an inversion centre are imperative. Among other issues, the effect of chirality of CNs on their NLO response awaits a thorough investigation.

## Acknowledgments

The author would like to thank Professor H Ajiki of Osaka University, Professor R Saito of Tokyo University of Electro-Communications and Professor H Yorikawa of Utsunomiya University for having sent the reprints of their papers on CNs.

## References

[1] Dresselhaus M S, Dresselhaus G and Eklund P C 1996 *Science of Fullerenes and Carbon Nanotubes* (San Diego, CA: Academic)
[2] Endo M, Iijima S and Dresselhaus M S (eds) 1996 *Carbon Nanotubes* (Oxford: Pergamon)
[3] Ebbesen T W 1995 *Annual Review of Material Science—Keynote Topic: Electronic Materials* vol 25, ed B Wessels *et al* (Palo Alto: Annual Reviews) p 235
[4] Ajayan P M and Ebbesen T W 1997 *Rep. Prog. Phys.* **60** 1025
[5] Blau W J, Byrne H J, Cardin D J, Dennis T J, Hare J P, Kroto H W, Taylor R and Walton D R M 1991 *Phys. Rev. Lett.* **67** 1423
[6] Wang Y and Cheng L T 1992 *J. Phys. Chem.* **96** 1530
[7] Wang Y, Bertsch G F and Tomanek D 1993 *Z. Phys.* D **25** 181
[8] Kinze P J and Partanen J P 1992 *Phys. Rev. Lett.* **68** 2704
[9] Meth J S, Vanherzeele H and Wang Y 1992 *Chem. Phys. Lett.* **197** 26
[10] Kafafi Z H, Bartoli F J, Lindle J R and Pong R G S 1992 *Phys. Rev. Lett.* **68** 2705
[11] Kafafi Z H, Lindle J R, Pong R G S, Bartoli F J, Lingg L J and Milliken J 1992 *Chem. Phys. Lett.* **188** 492
[12] Lascola R and Wright J S 1997 *Chem. Phys. Lett.* **269** 79
[13] Shuai Z and Brédas J L 1992 *Phys. Rev.* B **46** 16 135
[14] Shuai Z and Brédas J L 1993 *Synth. Met.* **56** 2973
[15] Takahashi A, Wang H X and Mukamel S 1993 *Chem. Phys. Lett.* **216** 394
[16] Harigaya K 1997 *Japan. J. Appl. Phys.* **36** L485
[17] Margulis Vl A and Sizikova T A 1998 *Physica* B **245** 173
[18] Genkin V M and Mednis P M 1968 *Zh. Eksp. Teor. Fiz.* **54** 1137 (Engl. transl. 1968 *Sov. Phys.–JETP* **37** 609)
[19] Mintmire J W, Dunlap B I and White C T 1992 *Phys. Rev. Lett.* **68** 631
[20] Saito R, Fujita M, Dresselhaus M S and Dresselhaus G 1992 *Phys. Rev.* B **46** 1804
[21] Saito R, Fujita M, Dresselhaus M S and Dresselhaus G 1992 *Appl. Phys. Lett.* **60** 2204
[22] Hamada N, Sawada S I and Oshiyama A 1992 *Phys. Rev. Lett.* **68** 1579
[23] Tanaka K, Okahara K, Okada M and Yamabe T 1992 *Chem. Phys. Lett.* **191** 469
[24] Yamabe T, Okahara K, Okada M and Tanaka K 1993 *Synth. Met.* **55–57** 3142
[25] Mintmire J M and White C T 1996 *Synth. Met.* **77** 231
[26] Yorikawa H and Muramatsu S 1996 *Synth. Met.* **82** 17
[27] Ajiki H and Ando T 1993 *J. Phys. Soc. Japan* **62** 1255
[28] Yorikawa H and Muramatsu S 1994 *Phys. Rev.* B **50** 12 203
[29] Yorikawa H and Muramatsu S 1995 *Phys. Rev.* B **52** 2723
[30] Yorikawa H and Muramatsu S 1995 *Solid State Commun.* **94** 435
[31] Ajiki H and Ando T 1996 *J. Phys. Soc. Japan* **65** 505
[32] Dresselhaus M S, Dresselhaus G and Saito R 1992 *Phys. Rev.* B **45** 6234
[33] Jishi R A, Venkataraman L, Dresselhaus M S and Dresselhaus G 1993 *Chem. Phys. Lett.* **209** 77
[34] Ducuing J 1977 *Nonlinear Spectroscopy* ed N Bloembergen (Amsterdam: North-Holland) p 276
[35] Margulis Vl A, Gaiduk E A and Zhidkin E N in preparation